

Spin-Hall effect in triplet chiral superconductors and graphene

K. Sengupta⁽¹⁾, Rahul Roy⁽²⁾, and Moitri Maiti⁽¹⁾

⁽¹⁾ *Theoretical Condensed Matter Physics Division and Center for Applied Mathematics and Computational Science Saha Institute of Nuclear Physics, 1/AF Bidhannagar, Kolkata-700064, India.*

⁽²⁾ *University of Illinois, Department of Physics, 1110 W. Green Street, Urbana, Illinois-61801, USA.*

(Dated: August 10, 2018)

We study spin-Hall effects in time-reversal symmetry (TRS) broken systems such as triplet chiral superconductors and TRS preserved ones such as graphene. For chiral triplet superconductors, we show that the edge states carry a quantized spin-Hall current in response to an applied Zeeman magnetic field B along the \mathbf{d} vector¹, whereas the edge spin-current for $\mathbf{B} \perp \mathbf{d}$ is screened by the condensate. We also derive the bulk spin-Hall current for chiral triplet superconductors for arbitrary relative orientation of \mathbf{B} and \mathbf{d} and discuss its relation with the edge spin-current. For TRS invariant system graphene, we show that the bulk effective action, unlike its TRS broken counterparts, does not support a SU(2) Hopf term but allows a crossed Hopf term in the presence of an external electromagnetic field, which yields a quantized bulk spin-Hall current in response to an electric field. We also present an analytical solution of the edge problem for armchair edges of graphene and contrast the properties of these edge states with their time reversal symmetry broken counterparts in chiral superconductors. We propose possible experiments to test our results.

PACS numbers: 73.43.-f, 73.61.Wp, 74.20.Rp, 74.70.Pq

I. INTRODUCTION

The generation and control of spin currents in various solid state systems have been an area of active research interest. Such systems can be broadly grouped into two categories; those which have broken time-reversal symmetry (TRS) and those which do not. Examples of the first group include chiral superfluids and superconductors such as two dimensional (2D) ³He-A films¹, 2D layered strontium ruthenate² and $d + id$ superconductor³. In these systems, the superfluid or superconducting order parameters break TRS and also provide a gap for the quasiparticle states at Fermi surface. Such a gap, together with broken TRS, naturally lead to chiral edge states and Hall effect^{4,5,6}. However, none of these systems support the usual charge Hall effect, since they are either charge neutral (³He-A) or do not have conserved physical charge density (ruthenates, $d + id$ superconductors)^{3,7}. Instead, they support spin and thermal Hall currents which were found to be quantized with $N = 2$ in $d + id$ systems³, and $N = 1$ in ³He-A and triplet superconductors^{8,9}. The second class of systems which do not break TRS but exhibit spin-Hall effect include doped semiconductors with spin-orbit interaction¹⁰ and graphene¹¹. In graphene, which provides a realization of Haldane's model¹², the spin-orbit interaction provides the gap for the effective low-energy Dirac-like Hamiltonian of the electrons near the Fermi (K and K') points¹¹. Such a gap breaks TRS individually for each spin species, but leaves the whole system invariant. Consequently, one expects a quantized charge Hall current j_s in the presence of an external electric field separately for the spin species $s = \uparrow, \downarrow$. These currents move in opposite directions so that $j_\uparrow = -j_\downarrow$. Thus the total charge Hall current vanishes; however, there exists a net spin-Hall current $j_{\text{spin}} = (j_\uparrow - j_\downarrow)\hbar/2e$. In the

absence of a Rashba term in the Hamiltonian, this spin current is exactly quantized with a spin-Hall conductivity $\sigma_s = e/2\pi$. In the presence of the Rashba term, where the number of up and down spin electrons are not conserved, the spin-Hall conductivity deviates from its quantized value¹³. This bulk picture of the spin-quantum Hall effect in graphene is further supported by numerical verification of the presence of chiral edge states at the boundaries of the 2D graphene sheet^{11,13}. It has also been shown that although the spin-Hall conductivity deviates from its quantized value, the spin-Hall effect and the edge states are robust against weak Rashba coupling^{13,14}.

The quantization of spin-Hall conductivity in both classes of such quasi 2D systems necessitates the existence of topological terms in their low energy bulk effective action. The nature of these topological terms depends crucially on whether the system is invariant under TRS or not. For systems with broken TRS, it has been shown that the low energy effective action has a SU(2) Hopf term which may lead to quantized spin-Hall current in the presence of an external magnetic field gradient^{3,8,9}. However, the details of the spin response of the triplet superconductors is expected to be qualitatively different from both singlet $d + id$ superconductors where the pair potential does not break spin-rotational symmetry, and ³He-A, which, being charge neutral, do not experience Meissner screening. A detailed understanding of the spin-current in triplet superconductors therefore requires an analysis of its effective action in the presence of an arbitrary Zeeman field. Such a study has not been undertaken so far. In contrast, for the second class of systems which respects TRS, one expects a crossed Hopf term¹⁵ which leads to a spin-Hall current in the presence of an external electric field. However, such a term has not been explicitly derived for graphene.

The presence/absence of TRS is also crucial for the

properties of the chiral edge states in these systems. Such states are well-known to exist for both triplet and singlet ($d + id$) chiral superconductors^{3,4,5,9}. In these systems, the edge modes corresponds to localized Bogoliubov quasiparticles states which have zero charge, but carry a finite charge current^{5,9}. For singlet $d + id$ superconductors, it is well known that the edge states also have a definite spin quantum number and would therefore carry a quantized spin-Hall current in the presence of an external magnetic field³. However, the spin structure of the edge states in triplet chiral superconductors has not been studied before. In contrast, for systems which preserves TRS, the edge modes, in the absence of external perturbations, can not carry any net charge current, but is expected to carry a finite non-quantized spin current^{11,12}. However, as we shall show, they can carry a experimentally detectable quantized charge current, if a population imbalance of spin-up and spin-down electrons is created at the edge.

The main results reported in this work are the following. First, for triplet chiral superconductors with the pair-potential given by

$$\Delta(\mathbf{k}) = \Delta_0 (\mathbf{s} \cdot \mathbf{d}) (k_x - ik_y) / k_F \quad (1)$$

where \mathbf{s} denotes Pauli matrices in spin-space, k_F denotes the Fermi wavevector, and \mathbf{d} denotes a direction in spin space orthogonal to the spin of the Cooper pair¹, we show that the spin structure of the chiral edge states is qualitatively different from the previously studied $d + id$ superconductors³. In particular, these edge states carry a quantized spin-current in response to an external magnetic field \mathbf{B} only if the external magnetic field is applied along the \mathbf{d} vector. The spin-current for $\mathbf{B} \perp \mathbf{d}$ is screened by Meissner current of the condensate. Second, we obtain an effective action for the bulk system in the presence of an arbitrary external Zeeman field, and derive an expression for bulk spin-current from this effective action for arbitrary relative orientation of the applied Zeeman field \mathbf{B} and \mathbf{d} . We compare this bulk spin-current with its edge counterpart for both $\mathbf{B} \parallel \mathbf{d}$ and $\mathbf{B} \perp \mathbf{d}$. In the limit of zero external Zeeman field our effective action reduces to those derived in Ref. 8,9 and contains an SU(2) Hopf term. Third, for the TRS invariant system graphene, starting from the low energy Dirac-like Hamiltonian¹¹, we derive an effective action in the presence of an external electromagnetic field, and show that it contains a crossed Hopf term¹⁵ which leads to a quantized spin-Hall current in response to an external electric field. We also include a weak Rashba term in the Hamiltonian^{11,12} and demonstrate that the spin-current deviates from its quantized value in the presence of such a term. Finally, we present a solution of the edge problem in graphene for the armchair edge and obtain analytical expressions for the energy dispersion and wavefunctions of the edge states. The properties of the edge states obtained from this analytical derivation matches previous numerical results^{11,12}. We also point out that these edge states can carry a quantized charge current in response

to an applied magnetic field which can be experimentally measured.

The organization of the paper is as follows. We discuss the properties of triplet chiral superconductors in Sec. II. In Sec. II A, we develop the edge state picture and discuss the spin structure of the edge states. This is followed by Sec. II B, where we obtain a bulk effective action for triplet chiral superconductors and derive an expression for the spin-Hall current in these systems. We compare the bulk spin-current with their edge counterparts for both $\mathbf{B} \parallel \mathbf{d}$ and $\mathbf{B} \perp \mathbf{d}$. Next, in Sec. III, we study spin-Hall effect in graphene. In Sec. III A, we derive a bulk effective action for graphene and show that a crossed Hopf term exists in its effective action which leads to an quantized spin-Hall conductivity in the absence of Rashba coupling. We also compute the deviation of this conductivity from its quantized value in the presence of a weak Rashba term in the Hamiltonian of the system. Next, in Sec. III B, we present an analytical solution for the edge state spectrum for the armchair edge and discuss the properties of these states. This is followed by a discussion of possible experiments and concluding remarks in Sec. IV.

II. CHIRAL TRIPLET SUPERCONDUCTORS

For triplet superconductors, Cooper-pairing occurs in the $L = 1$, $S = 1$ channel, and consequently the pair-potential (Eq. 1) breaks spin-rotational invariance. This is manifested in the presence of the \mathbf{d} vector in the expression of the pair-potential (Eq. 1) which refers to a direction orthogonal to the direction of the spin \mathbf{S} of the Cooper pair, so that a choice of spin quantization axis along \mathbf{d} implies opposite-spin pairing¹. In the presence of such a pair potential, the action for chiral superconductors can be written as

$$S = \int d^2r dt \psi^\dagger(t, \mathbf{r}) \left[i\partial_t - \tau_3(\epsilon(-i\nabla) - E_F) - \tau_+ \Delta(\mathbf{k}) - \tau_- \Delta^*(\mathbf{k}) \right] \psi(t, \mathbf{r}), \quad (2)$$

where τ denotes Pauli matrices acting in particle-hole space, $\epsilon(\mathbf{k}) = (k_x^2 + k_y^2)/2m$ is the kinetic energy, $\psi = (\psi_s, g_{ss'} \psi^{\dagger s'})$, for spin indices $s, s' = \uparrow, \downarrow$, is the four component Pauli spinor, and $g_{ss'} = i(s_y)_{ss'}$ is the metric tensor in spin space⁸. Notice that under time-reversal symmetry $\Delta(k_x, k_y) \rightarrow \Delta(-k_x, k_y)$ and thus the pair-potential breaks time reversal symmetry. We shall use this action to analyze the edge and the bulk properties of the system in Secs. II A and II B.

A. Edge states

In this section, we analyze the spin properties of the edge states. We shall assume that the \mathbf{d} vector is fixed

along a specific direction due to the spin-orbit interaction throughout the superconductors. This is expected to be the case for layered chiral superconductors Sr_2RuO_4 where the \mathbf{d} vector is fixed along c -axis perpendicular to the Ru – O plane¹⁶. In this section, we shall adapt the following convention for the choice of spin-quantization axis for the electrons: if an external magnetic field is applied, the spin-quantization will be chosen along the field; else it will be chosen to be along \mathbf{d} . For the rest of this work, we shall choose $\hbar = c = 1$, unless explicitly mentioned.

First, we consider the edge problem in absence of the Zeeman field. Here we shall consider a semi-infinite sample with an edge at $x = 0$ and assume a step-function dependence of the pair-potential¹⁷. In this case, the Bogoliubov-de Gennes (BdG) equation can be written as

$$\begin{pmatrix} \mathcal{H}_0 & \Delta(\mathbf{k}_F)s_z \\ \Delta^*(\mathbf{k}_F)s_z & -\mathcal{H}_0 \end{pmatrix} \Psi(x, k_{Fy}) = E\Psi(x, k_{Fy}), \quad (3)$$

where $\mathcal{H}_0 = \epsilon(-i\partial_x, k_y) - E_F = -iv_F\partial_x$ is the linearized dispersion and k_{Fy} is the in-plane momentum component of the Fermi surface along the edge, and $\Psi(x, k_{Fy}) = (u_s(x, k_{Fy}), i(\sigma_y)_{ss'}v_{s'}(x, k_{Fy}))$ is the four-component spinor wavefunction. It is well-known that in the presence of an edge which enforces a boundary condition $\Psi(x=0, k_{Fy}) = 0$, Eq. 3 admits localized chiral edge states^{4,9,16,17}

$$\begin{aligned} \Psi(x, k_{Fy}) &= 2i\sqrt{\kappa}e^{ik_{Fy}y}e^{-\kappa x} \sin(k_{Fx}x) \begin{pmatrix} u_s \\ \text{sgn}(s)v_{\bar{s}} \end{pmatrix}, \\ E(k_{Fy}) &= \frac{\Delta_0 k_{Fy}}{k_F}, \quad \kappa = \frac{\Delta_0}{k_F v_F} k_{Fx}, \end{aligned} \quad (4)$$

where $\text{sgn}(s) = \pm$ for $s = \uparrow\downarrow$, $u_s = \exp(i\theta_b)v_{\bar{s}}$, θ_b is the global U(1) phase of the pair-potential Δ , and $u_{\uparrow\downarrow}$ are the coefficients of spin-up and spin-down components of the normalized single-particle wavefunctions with $|u_s|^2 + |v_{\bar{s}}|^2 = 1$. These chiral edge quasiparticles are BCS quasiparticles with equal proportion of spin s electrons and spin \bar{s} holes; consequently, they do not carry any charge but have a well defined a spin quantum number $\text{sgn}(s)/2$ along \mathbf{d} . They have a group velocity $v_e = \partial E(k_{Fy})/\partial k_{Fy} = \Delta_0/k_F$ and carry a charge current^{9,16,18}

$$I_{\text{edge}}^{\text{charge}} = \sum_{k_{Fy}, s} \frac{ek_{Fy}}{m} n_s(k_{Fy}) = \frac{ek_F^2}{4\pi m}, \quad (5)$$

where $n_s(k_{Fy}) = \theta(k_F - k_{Fy})$ is the density of states for edge state with spin $\text{sgn}(s)/2$ at zero temperature. The charge current is not carried with group velocity and is not quantized. The presence of such a charge current at the edge of a superconductor also leads to Meissner screening current by the condensate, so that the sum of magnetic fields due to both the currents vanish at the bulk of the superconductor^{6,18,19}.

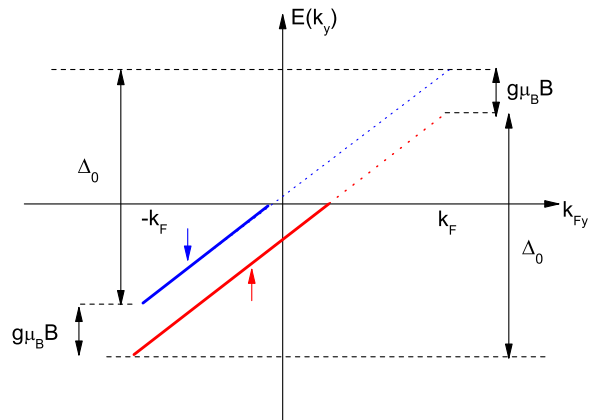


FIG. 1: Chiral edge states in spin triplet superconductors in the presence of a Zeeman magnetic field B along \mathbf{d} . The red (blue) solid lines denote occupied spin-up (spin-down) edge states while the corresponding dotted lines show the unoccupied states. The dashed black lines are guide to the eye.

In the absence of any external Zeeman magnetic field, the spin-up and spin-down edge quasiparticle states are equally populated and hence the spin-current carried by them cancels. Now, let us apply a Zeeman magnetic field B along \mathbf{d} so that (choosing the spin-quantization axis along B and \mathbf{d}) the BdG equations for the edge quasiparticles states can be written as

$$\begin{pmatrix} \mathcal{H}_0 - g\mu_B B s_z & \Delta(\mathbf{k}_F)s_z \\ \Delta^*(\mathbf{k}_F)s_z & -(\mathcal{H}_0 + g\mu_B B s_z) \end{pmatrix} \Psi(x, k_{Fy}) = E\Psi(x, k_{Fy}), \quad (6)$$

where μ_B is the Bohr magneton and g denotes the gyromagnetic ratio. We note that here the effect of the magnetic field is to shift the energies of the spin-up and spin-down states in *opposite* direction: $E_s(k_{Fy}) = \Delta_0 k_{Fy}/k_F - \text{sgn}(s)g\mu_B B$. As a result, there is an imbalance in the population of the spin-up and spin-down quasiparticle states as shown in Fig. 1 which leads to a net quantized edge spin-current

$$(I_{\parallel}^z)_{\text{edge}}^{\text{spin}} = \frac{1}{2}v_e(N_{\uparrow} - N_{\downarrow}) = \frac{1}{8\pi}g\mu_B B. \quad (7)$$

Note that the spin current, in contrast to the charge current, is associated with the group velocity v_e of the edge states. Further with our choice of spin-quantization axis (along \mathbf{d}), the condensate comprises of Cooper pairs with *opposite spin pairing*. Hence the condensate do not carry any spin or spin-current and can not screen the edge spin-current.

Such a quantized spin current in the presence of external Zeeman field is also carried by edge states in singlet $d + id$ superconductors regardless of the direction of the applied magnetic field. The situation for the triplet superconductors is different as we now show by studying

the spin response of the edge states in the presence of the Zeeman field applied perpendicular to \mathbf{d} . Here, without loss of generality, we choose $\mathbf{d} = \hat{y}$ and take the spin-quantization axis along $\mathbf{H} = H\hat{z}$. The BdG equation can now be written as

$$\begin{pmatrix} \mathcal{H}_0 - g\mu_B B s_z & \Delta(\mathbf{k}_F)_{s_y} \\ \Delta^*(\mathbf{k}_F)_{s_y} & -(\mathcal{H}_0 - g\mu_B B s_z) \end{pmatrix} \Psi(x, k_{Fy}) = E \Psi(x, k_{Fy}). \quad (8)$$

One immediately notes that in this case, the magnetic field does not shift the energy of the edge states, but shifts the Fermi wave-vector for the spin-up and spin-down quasiparticles in opposite directions: $k_{Fs} = \sqrt{k_F + \text{sgn}(s)2mg\mu_B B}$. The BCS quasiparticles are now equal superposition of electron and hole states with the *same spin* s . As a result, just as in the case of charge, they do not carry a spin quantum number along z : $\langle s_z \rangle \equiv (|u_s|^2 - |v_s|^2) = 0$. The edge states now carry a net charge current

$$\begin{aligned} (I_{\perp})_{\text{edge}}^{\text{charge}} &= \sum_s (I_{s,\perp})_{\text{edge}}^{\text{charge}}, \\ (I_{s,\perp})_{\text{edge}}^{\text{charge}} &= \sum_{k_{Fy}=0}^{k_{Fs}} e \frac{\hbar k_{Fy}}{m} n_s(k_{Fy}) = \frac{e k_{Fs}^2}{8\pi m}. \end{aligned} \quad (9)$$

Now let us consider Meissner screening of this charge current. Since we have chosen the direction of spin quantization axis perpendicular to the \mathbf{d} vector, we have equal spin pairing in the bulk ($\Delta_{\uparrow\uparrow} = \Delta_{\downarrow\downarrow} = \Delta$) and hence the Cooper pairs carry a net $s_z = \pm\hbar$. In the presence of a Zeeman magnetic field, the spin-up and the spin-down condensates see a shifted chemical potential $\mu_{\uparrow\downarrow} = \mu \pm g\mu_B B$. In this situation, one can apply the arguments of Refs. 5,19 in a straightforward manner and show that the edge currents would be screened by spontaneously generated Meissner current

$$\begin{aligned} I^{\text{Meissner}} &= \sum_s I_s^{\text{Meissner}}, \\ I_s^{\text{Meissner}} &= -(I_{s,\perp})_{\text{edge}}^{\text{charge}}, \end{aligned} \quad (10)$$

so as to cancel the net magnetic field due to the edge currents in the bulk.

The edge states now also carry a net spin current, since the electron and holes with spin s constituting the BCS quasiparticles have opposite velocities. In the presence of an external Zeeman field $\mathbf{B} \perp \mathbf{d}$, $k_{F\uparrow}$ and $k_{F\downarrow}$ are different, and consequently the net spin-current is given by

$$(I_{\perp}^z)_{\text{edge}}^{\text{spin}} = \frac{1}{2e} \sum_s \text{sgn}(s) (I_{s,\perp})_{\text{edge}}^{\text{charge}} = \frac{g\mu_B B}{8\pi}. \quad (11)$$

Notice that the spin current is not carried by the group velocity. Further, since the condensate now carry a net

spin, the Meissner current generated as the response to edge charge current also carry a net spin-current

$$\begin{aligned} I_{\text{Meissner}}^{\text{spin}} &= \frac{1}{2e} \sum_s \text{sgn}(s) I_s^{\text{Meissner}}, \\ &= -\frac{1}{2e} \sum_s \text{sgn}(s) (I_{s,\perp})_{\text{edge}}^{\text{charge}}, \\ &= -(I_{\perp}^z)_{\text{edge}}^{\text{spin}}. \end{aligned} \quad (12)$$

Thus the edge spin current generated by the response of a magnetic external Zeeman field $\mathbf{B} \perp \mathbf{d}$ is screened by the condensate, analogous to the charge current. Therefore the response of the edge states to an applied Zeeman field in triplet chiral superconductors depends crucially on the direction of the applied field. We shall discuss possible experiments to probe this behavior in Sec. IV.

Before ending this section, we note that all of the results derived can be applied to ruthenates where the pair-potential is expected to have horizontal line of nodes with the substitution $\Delta \rightarrow \Delta |\cos(ck_z)|^{20}$. In particular, it can be shown that the spin response of the edge states remain qualitatively similar in the presence of such horizontal line of nodes.

B. Bulk effective action

To derive the bulk effective action, we begin with the action of chiral triplet superconductors in the presence of an external Zeeman field $B(t, \mathbf{r})$ and an arbitrary \mathbf{d} field configuration. In the presence of such a term the action can be written as

$$\begin{aligned} S &= \int d^2r dt \psi^\dagger(t, \mathbf{r}) \left[i\partial_t - C_0^{\text{ext}} \right. \\ &\quad \left. - \tau_3(\epsilon(-i\partial_i - C_i^{\text{ext}}) - E_F) - \tau_+ \Delta(-\partial_i - C_i^{\text{ext}}) \right. \\ &\quad \left. - \tau_- \Delta^*(-i\partial_i - C_i^{\text{ext}}) \right] \psi(t, \mathbf{r}), \end{aligned} \quad (13)$$

where $C_0^{\text{ext}} = g\mu_B \mathbf{s} \cdot \mathbf{B}(t, \mathbf{r})$ is the Zeeman field and Δ is the pair-potential defined in Eq. 1. Here, and in the rest of this section, we shall use the notation $\partial_\mu = (\partial_t, \partial_x, \partial_y)$ and adapt the sign convention that all covariant vectors have $F_\mu = (F_t, -F_x, -F_y)$ and all operators have $\partial_\mu = (\partial_t, \partial_x, \partial_y)$. The corresponding contravariant vectors and operators can be obtained by applying the metric tensor $g_{\mu\nu} = g^{\mu\nu} = (1, -1, -1)$. Also, here we have followed Ref. 8 to treat the Zeeman magnetic field as the time component of an external SU(2) gauge field $C_\mu^{\text{ext}} = 1/2s_\alpha \cdot \Omega_\mu^{\alpha \text{ext}}$ with $\Omega_t^{\text{ext}} = g\mu_B \mathbf{B}$. The spatial component of C_μ^{ext} are fictitious fields which shall be set to zero at the end of the calculation. The advantage of introducing these fictitious gauge fields becomes apparent when we note that the spin-current can be obtained

using these fields as

$$\begin{aligned} j_i^\alpha &= \left\langle \psi'^{\dagger} \frac{1}{2} \left\{ \partial_{k_\mu} G_0^{-1}(k), s^\alpha \right\}_+ \psi'(k) \right\rangle_S, \\ &= \frac{\delta S_{\text{eff}}}{\delta \Omega_i^{\alpha \text{ ext}}} \Big|_{\Omega_i^{\alpha \text{ ext}}=0}, \end{aligned} \quad (14)$$

where S_{eff} is the effective action obtained by integrating out Fermions in S (Eq. 13).

Next we introduce a $SU(2)$ rotation in spin space through the transformation $\psi(t, \mathbf{r}) \rightarrow \psi'(t, \mathbf{r}) = U^\dagger \psi(t, \mathbf{r})$, so that the local $SU(2)$ rotation matrix rotates the \mathbf{d} vector to z : $U^\dagger (\mathbf{s} \cdot \mathbf{d}) U = s_z$. One can now write the action as

$$S = S_0 + S_1, \quad (15)$$

$$S_0 = \int \frac{d^2 k d\omega}{(2\pi)^3} \psi'^{\dagger}(k) G_0^{-1} \psi'(k), \quad (16)$$

$$\begin{aligned} S_1 &= - \int \frac{d^2 k d^2 p d\omega dp_0}{(2\pi)^6} \psi'^{\dagger}(k+p) \\ &\quad \times \frac{1}{2} \left\{ \partial_{k_\mu} G_0^{-1}(k), C_\mu^{\text{total}}(p) \right\}_+ \psi'(k), \end{aligned} \quad (17)$$

where the notation $\{..\}_+$ denotes anticommutation, the Green function $G_0(k)$ is given by

$$G_0(k; \Delta_0) = \frac{\omega + \tau_3 (\epsilon(\mathbf{k}) - E_F) + \Delta_0 (\mathbf{k} \cdot \boldsymbol{\tau}) s_z}{\omega^2 - E_k^2 + i\eta}, \quad (18)$$

$$E_k = \sqrt{(\epsilon(\mathbf{k}) - E_F)^2 + \Delta_0^2}, \quad (19)$$

and the gauge fields C_μ^{total} are given by

$$\begin{aligned} C_\mu^{\text{total}} &= U^\dagger C_\mu^{\text{ext}} U + C_\mu^{\text{int}}, \\ C_\mu^{\text{int}} &= -iU^\dagger \partial_\mu U = \frac{1}{2} s_\alpha \Omega_\mu^{\alpha \text{ int}}. \end{aligned} \quad (20)$$

Note that here the internal gauge fields C_μ^{int} are 'pure' gauge fields in the sense that they satisfy

$$\partial_\mu \boldsymbol{\Omega}_\nu^{\text{int}} - \partial_\nu \boldsymbol{\Omega}_\mu^{\text{int}} - \boldsymbol{\Omega}_\mu^{\text{int}} \times \boldsymbol{\Omega}_\nu^{\text{int}} = \mathbf{f}_{\mu\nu}^{\text{int}} = 0. \quad (21)$$

These fields are small when the \mathbf{d} fields are slowly varying. Thus for a slowly-varying configuration of both \mathbf{d} field and external Zeeman field \mathbf{B} , one can carry out a gradient expansion in C_μ^{total} . To this end, we now integrate out the fermions fields from S and carry out a gradient expansion of the resultant effective action in C_μ^{total} as done in Refs. 8,9,22. We shall concentrate here only on the terms in the effective action which contributes to the spin-Hall current. These diagrams are shown in Fig. 2. After some straightforward, but tedious algebra, one obtains the effective action which has the same form as

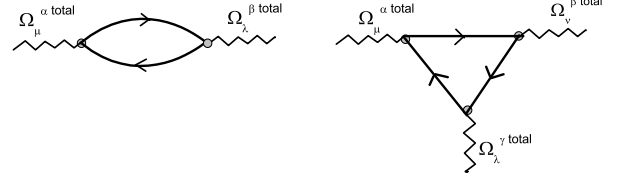


FIG. 2: Feynman diagrams which contribute to the $SU(2)$ Hopf terms effective action. The closed circles represent $1/2 \left\{ \partial G_0^{-1} / \partial k_b, s_i \right\}_+$ with $b = \mu, \nu$ or λ and $i = \alpha, \beta$ or γ as appropriate. The space-time indices μ, ν and λ take values t, x and y whereas the spin indices α, β and γ take values x, y and z . The straight lines denote the Green function G_0 and the wavy lines denote the total $SU(2)$ gauge fields Ω^{total}

that obtained for $^3\text{He-A}$ in Ref. 8

$$S_{\text{eff}} = S_{\text{int}} + S_{\text{ext}} + S_{\text{coupling}}, \quad (22)$$

$$S_{\text{int}} = \frac{N}{16\pi} \epsilon_{\mu\nu\lambda} \int d^2 r dt \Omega_\nu^{\text{int}} \partial_\lambda \Omega_\mu^{\text{int}}, \quad (23)$$

$$\begin{aligned} S_{\text{ext}} &= \frac{N}{32\pi} \epsilon_{\mu\nu\lambda} \int d^2 r dt \left[\boldsymbol{\Omega}_\mu^{\text{ext}} \cdot \mathbf{f}_{\nu\lambda}^{\text{ext}} \right. \\ &\quad \left. - \frac{1}{3} \boldsymbol{\Omega}_\mu^{\text{ext}} \cdot (\boldsymbol{\Omega}_\nu^{\text{ext}} \times \boldsymbol{\Omega}_\lambda^{\text{ext}}) \right], \end{aligned} \quad (24)$$

$$\begin{aligned} S_{\text{coupling}} &= \frac{1}{16\pi} \int d^2 r dt \left[N \epsilon_{\mu\nu\lambda} \right. \\ &\quad \times (\partial_\mu \mathbf{d} - \boldsymbol{\Omega}_\mu^{\text{ext}} \times \mathbf{d}) \cdot (\mathbf{f}_{\nu\lambda}^{\text{ext}} \times \mathbf{d}) \\ &\quad \left. + 2P (\partial_t \mathbf{d} - \boldsymbol{\Omega}_t^{\text{ext}} \times \mathbf{d}) \cdot (\mathbf{f}_{xy}^{\text{ext}} \times \mathbf{d}) \right]. \end{aligned} \quad (25)$$

Here $\mathbf{f}_{\mu\nu}^{\text{ext}} = \partial_\mu \boldsymbol{\Omega}_\nu^{\text{ext}} - \partial_\nu \boldsymbol{\Omega}_\mu^{\text{ext}} - \boldsymbol{\Omega}_\mu^{\text{ext}} \times \boldsymbol{\Omega}_\nu^{\text{ext}}$ is the field-strength corresponding to the external $SU(2)$ fields, $\epsilon_{\mu\nu\lambda}$ is the antisymmetric tensor and the coefficients N and P can be written in terms of the Green function $G_0(k; \Delta_0)$ as^{8,9}

$$\begin{aligned} N &= 2\pi \text{Tr} \left[G_0(k; \Delta_0) \frac{\partial G_0^{-1}(k, \Delta_0)}{\partial k_x} G_0(k; \Delta_0) \right. \\ &\quad \left. \times \frac{\partial G_0^{-1}(k, \Delta_0)}{\partial k_y} G_0(k; \Delta_0) \frac{\partial G_0^{-1}(k, \Delta_0)}{\partial \omega} \right], \end{aligned} \quad (26)$$

$$\begin{aligned} P &= 2\pi \text{Tr} \left[G_0(k; \Delta_0) \frac{\partial G_0^{-1}(k; \Delta_0)}{\partial \omega} G_0(k; \Delta_0) \right. \\ &\quad \left. \times \frac{\partial G_0^{-1}(k; 0)}{\partial k_x} G_0(k; -\Delta_0) \frac{\partial G_0^{-1}(k, 0)}{\partial k_y} \right], \end{aligned} \quad (27)$$

where Tr denotes matrix traces and sum over all frequencies and momenta. Notice that N is precisely the topological invariant that characterizes the $SU(2)$ Hopf term as shown in Refs. 8,9. For chiral triplet p -wave superconductors and $^3\text{He-A}$, it is well-known that $N = 1$. The

coefficient P , however, is not a topological invariant and its numerical value depends on the details of the system. Evaluating the integrals and matrix traces in Eq. 27, one finds that $P = 1$ as long as we restrict ourselves to clean systems and $T = 0$. In this work, we shall restrict ourselves within this domain. We also note that N is exactly quantized only if there are no nodes in the superconducting gap; however, the deviation of N from its quantized value is expected to be vanishingly small in ruthenates in the presence of the line of nodes, since the gap vanishes only along a line of the entire three dimensional Fermi surface. We shall ignore such deviation in the rest of this section.

In the absence of external Zeeman field, we are left with only the internal fields $\mathbf{\Omega}_\mu^{\text{int}}$. In this case, the effective action $S_{\text{eff}} = S_{\text{int}}$ (Eqs. 22,23) reduces to SU(2) Hopf term derived in Refs. 8,9. The contribution to the spin-current, on the other hand, comes from S_{coupling} and S_{ext} , and thus requires the full effective action in the presence of a finite Zeeman field. Using Eqs. 14, 24, and 25, we obtain the spin-Hall current for arbitrary configuration of the $\mathbf{d}(\mathbf{r}, t)$ and for any relative orientation of the applied Zeeman field \mathbf{B} and \mathbf{d}

$$\mathbf{j}_i(\mathbf{r}, t) = \frac{1}{8\pi} \epsilon_{ij} \left[\partial_j \left\{ P \gamma \mathbf{B} - \frac{1}{2} (N + 2P) \mathbf{d} (\mathbf{d} \cdot \gamma \mathbf{B}) \right\} - 2N \partial_j (\mathbf{d} \times \partial_t \mathbf{d}) - \frac{N}{2} \mathbf{d} \partial_j (\mathbf{d} \cdot \gamma \mathbf{B}) \right], \quad (28)$$

where i and j takes values x, y , $\gamma = g\mu_B$, and ϵ_{ij} is the antisymmetric tensor with $\epsilon_{xy} = 1$. Note that Eq. 28 has to be supplemented with the equation governing the dynamics of the \mathbf{d} fields in the presence of an external magnetic field. This has been derived, in the presence of a pinning term, in Ref. 23. For the rest of this section, we shall concentrate on the case where the pinning potential (and hence the pinning frequency) is larger than all other scales in the problem, so that \mathbf{d} is fixed along the c-axis.

First, let us consider the case when $\mathbf{B} \parallel \mathbf{d} = B\hat{z}$. In this case one obtains a quantized spin-Hall bulk current from Eq. 28

$$(j_i^z)^\parallel = -\frac{N}{8\pi} \epsilon_{ij} \partial_j (g\mu_B B) = -\frac{1}{8\pi} \epsilon_{ij} \partial_j (g\mu_B B). \quad (29)$$

This result differs from the conclusion of Ref. 8, where the bulk spin current is claimed to vanish for magnetic field along the \mathbf{d} vector. To understand the reason for this difference, let us consider a superconducting sample occupying semi-infinite space $x \geq 0$ with an edge at $x = 0$. In this case, since magnetic field B decays to zero deep inside the superconductor, the bulk spin-current is given by

$$\begin{aligned} (I_y^z)^\parallel_{\text{bulk}} &= \int_0^\infty (j_y^z)^\parallel dx \\ &= -\frac{1}{8\pi} (g\mu_B B) = -(I_\parallel^z)^{\text{spin}}, \end{aligned} \quad (30)$$

where $(I_\parallel^z)^{\text{spin}}$ is the edge spin current given by Eq. 7. Thus the bulk spin current is *equal and opposite* to the edge current. This has an interesting consequence. Imagine that we place the semi-infinite sample with a solenoid coil centered around the edge of the sample at $x = 0$ which produces a magnetic field along \mathbf{d} . In this case, the solenoid will create a both a bulk and the edge spin current so that total spin current $(I_\parallel^z)^{\text{spin}} + (I_y^z)^\parallel_{\text{bulk}} = 0$. This is due to the fact that the solenoid creates a potential difference but no net electrochemical potential difference in the sample. Consequently, any net transverse spin-current must vanish. This effect is analogous to the well-known absence of charge quantum Hall current when a semiconducting sample is placed between the plates of a capacitor. Thus we conclude that, contrary to the claim in the Ref. 8, the bulk spin current does not vanish for $\mathbf{B} \parallel \mathbf{d}$; however the bulk and the edge spin current do cancel out each other, and the total spin-current vanishes. Also note that in this case the orbital effect of the magnetic field, which we have neglected so far, do not contribute to the spin-current since the condensate do not carry any net spin.

In contrast, when the magnetic field is applied perpendicular to the \mathbf{d} vector (we choose $\mathbf{B} = B\hat{z}$ and $\mathbf{d} \parallel \hat{y}$), the bulk spin-current becomes

$$\begin{aligned} (I_y^z)^\perp_{\text{bulk}} &= \int_0^\infty (j_y^z)^\perp dx \\ &= \frac{P}{8\pi} (g\mu_B B) = \frac{1}{8\pi} (g\mu_B B). \end{aligned} \quad (31)$$

Thus we find that there is a net bulk spin-Hall current for $\mathbf{B} \perp \mathbf{d}$ which is in accordance with the conclusion of Ref. 8. Notice that in this case, as we have seen in the Sec. II A, the edge spin current is already screened by the Meissner current and hence it does not contribute to the net spin current. By taking into account the generation of Meissner current, we have qualitatively taken into account the orbital effect of the applied magnetic field. A detailed numerical computation, following the lines of Ref. 5, is required to address this issue on a more quantitative level and is beyond the scope of the present work. Also, we note that $(I_y^z)^\perp_{\text{bulk}}$ depends on P and not the SU(2) Hopf coefficient N , as can be easily seen from Eq. 28. Thus we conclude that the bulk spin-Hall conductivity in a triplet chiral superconductor (and also $^3\text{He-A}$) for $\mathbf{B} \perp \mathbf{d}$ is not truly quantized, although for clean systems at $T = 0$ where $P = 1$, it reaches its quantized value $1/8\pi$.

III. GRAPHENE

The low energy Hamiltonian of graphene, in the presence of Rashba coupling, is given by¹¹

$$H = \int d^2r \psi^\dagger(\mathbf{r}) \left[-iv_F (\tau_z \sigma_x \partial_x + \sigma_y \partial_y) + \Delta_1 \tau_z \sigma_z s_z + \lambda_R (\tau_z s_y \sigma_x - s_x \sigma_y) \right] \psi(\mathbf{r}), \quad (32)$$

where v_F is the Fermi velocity, τ_i , σ_i and s_i are the Pauli matrices in the $K - K'$, $A - B$ and spin spaces respectively, Δ_1 is the spin-orbit coupling gap, and λ_R denotes the Rashba coupling. Note that the spin-orbit coupling gap does not break time reversal symmetry on the whole, but does so for each individual spin species. Here ψ is a 8 component fermionic spinor field given by $\psi = (\psi_{A\uparrow}^K, \psi_{B\uparrow}^K, \psi_{A\uparrow}^{K'}, \psi_{B\uparrow}^{K'}, \psi_{A\downarrow}^K, \psi_{B\downarrow}^K, \psi_{A\downarrow}^{K'}, \psi_{B\downarrow}^{K'})$. In the rest of this section, we shall analyze this Hamiltonian in the presence of an weak external electromagnetic field, and also study its energy spectrum in the presence of an armchair edge. Our derivation can in principle to other models for spin-Hall effect which has similar structure of the effective low-energy Hamiltonian²¹

A. Bulk effective action

In this section, we derive a low energy effective action of graphene in the presence of an external electromagnetic field and obtain the expression of spin-current from that effective action. First, we study the system in the absence of Rashba coupling. We begin with the action

$$S = \int d^2r dt \psi^\dagger(\mathbf{r}, \tau) \left[i\partial_t - eA_0 - v_F (\tau_z \sigma_x (-i\partial_x - eA_x) + \sigma_y (-i\partial_y - eA_y)) - \Delta_1 \tau_z \sigma_z \mathbf{s} \cdot \mathbf{d}(\mathbf{r}, t) \right] \psi(\mathbf{r}, \tau), \quad (33)$$

where A_μ denotes the $U(1)$ gauge fields corresponding to an external electric field $E_i = -\partial_t A_i - \partial_i A_0$. Note that here we have introduced an unit vector field $\mathbf{d}(\mathbf{r}, \tau)$. The Hamiltonian H (Eq. 32) corresponds to the configuration $\mathbf{d} = z$ and we shall set $\mathbf{d} = z$ at the end of the calculation.

Next, as in Sec. II B, we introduce a $SU(2)$ rotation in the spin-space $\psi(\mathbf{r}, \tau) \rightarrow \psi'(\mathbf{r}, \tau) = U^\dagger \psi(\mathbf{r}, \tau)$ where U is a local $SU(2)$ rotation matrix which rotates the local \mathbf{d} vector to z : $U^\dagger \mathbf{s} \cdot \mathbf{d} U = s_z$. The partition function can now be written in terms of the new spinor fields $\psi'(k) \equiv$

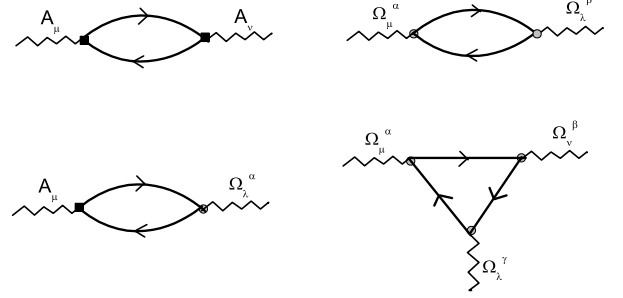


FIG. 3: Feynman diagrams which contribute to the possible Hopf terms effective action. The left panel contains diagram contributing to $S^{(1)}$ and $S^{(2)}$ whereas the right panel shows diagrams contributing to $S^{(2)}$. The filled squares represent the vertices $\partial G_0^{-1}/\partial k_b$ with $b = \mu$ or ν , as appropriate. The closed circles represent $1/2 \{\partial G_0^{-1}/\partial k_b, s_i\}_+$ as in Fig. ??, whereas the straight lines denote the Green function G_0 .

$\psi'(\mathbf{k}, \omega)$

$$Z = \int \mathcal{D}\psi'^\dagger \mathcal{D}\psi' \mathcal{D}C_\mu \mathcal{D}A_\mu \exp[i(S_0 + S_1)], \quad (34)$$

$$S_0 = \int \frac{d^2k d\omega}{(2\pi)^3} \psi'^\dagger(k) G_0^{-1}(k) \psi'(k),$$

$$S_1 = - \int \frac{d^2k d^2p d\omega dp_0}{(2\pi)^6} \psi'^\dagger(k+p) \times \frac{1}{2} \{ \partial_{k_\mu} G_0^{-1}(k), eA_\mu(p) + C_\mu(p) \}_+ \psi'(k), \quad (35)$$

where the fields $C_\mu = -iU^\dagger \partial_\mu U = 1/2 \mathbf{s} \cdot \boldsymbol{\Omega}_\mu$ are the $SU(2)$ gauge fields, the configuration $\mathbf{d} = z$ corresponds to $C_\mu = 0$ and we have used the same notations as in Sec. II B. Here the Green function $G_0(k; \Delta_1)$ is given by

$$G_0(k; \Delta_1) = \frac{\omega + v_F (\tau_3 k_x \sigma_x + k_y \sigma_y) + \Delta_1 \tau_z \sigma_z s_z}{\omega^2 - E_k^2 + i\eta}, \quad (36)$$

$$E_k = \sqrt{v_F^2 (k_x^2 + k_y^2) + \Delta_1^2}.$$

Note that the ψ' fields see a gap term $\Delta_1 \sigma_z \tau_z s_z$ and therefore describes the same action as the one corresponding to H (Eq. 32) in the absence of the C_μ fields. The advantage of introducing the \mathbf{d} fields now become clear, since we find that the spin-current density $j_\mu^\alpha = \langle \psi'^\dagger \frac{1}{2} \{ \partial_{k_\mu} G_0^{-1}(k), s^\alpha \}_+ \psi' \rangle$ can be obtained as

$$j_\mu^\alpha = \left. \frac{\partial S_{\text{eff}}[C_\mu, A_\mu]}{\partial \Omega_\mu^\alpha} \right|_{\Omega_\mu^\alpha=0}, \quad (37)$$

where S_{eff} is the effective action obtained by integrating out the Fermion fields. Here the $\mu = t$ component of the spin-current is simply the spin-density $\mathbf{j}_t = \langle \psi'^\dagger \mathbf{s} \psi' \rangle$.

To obtain the effective action, we now integrate out the fermionic fields and compute the effective action for A_μ

and C_μ fields. Since for slowly varying \mathbf{d} field configuration C_μ is small, we can carry out a gradient expansion in powers of the fields A_μ and C_μ and their derivatives in a straightforward manner. The relevant terms in the effective action which contributes to the Hopf terms comes from the first derivative of the polarization bubble and triangle diagram shown in Fig. 3. These terms are given by

$$S_{\text{eff}}[A_\mu, C_\mu] = S^{(1)} + S^{(2)} + S^{(3)}, \quad (38)$$

$$S^{(1)} = a_{\mu\nu\lambda} \int d^2r dt A_\nu \partial_\lambda A_\mu, \quad (39)$$

$$S^{(2)} = b_{\mu\nu\lambda}^{\alpha\beta} \int d^2r dt \Omega_\nu^\alpha \partial_\lambda \Omega_\mu^\beta + c_{\mu\nu\lambda}^{\alpha\beta\gamma} \int d^2r dt \Omega_\mu^\alpha \Omega_\nu^\beta \Omega_\lambda^\gamma, \quad (40)$$

$$S^{(3)} = d_{\mu\nu\lambda}^\alpha \int d^2r dt A_\nu \partial_\lambda \Omega_\mu^\alpha, \quad (41)$$

where we have used the definition $C_\mu = 1/2s_\alpha \Omega_\mu^\alpha$, and all repeated indices are summed over. The coefficients of the terms in the effective action can be expressed in terms of Green functions as

$$a_{\mu\nu\lambda} = -\frac{e^2}{2} \text{Tr} \left(\frac{\partial G_0^{-1}}{\partial k_\mu} G_0(k; \Delta_1) \frac{\partial G_0^{-1}}{\partial k_\nu} \times G_0(k; \Delta_1) \frac{\partial G_0^{-1}}{\partial k_\lambda} G_0(k; \Delta_1) \right), \quad (42)$$

$$b_{\mu\nu\lambda}^{\alpha\beta} = -\frac{1}{8} \text{Tr} \left(\left\{ \frac{\partial G_0^{-1}}{\partial k_\mu}, s_\alpha \right\}_+ G_0(k; \Delta_1) \left\{ \frac{\partial G_0^{-1}}{\partial k_\nu}, s_\beta \right\}_+ \times G_0(k; \Delta_1) \frac{\partial G_0^{-1}}{\partial k_\lambda} G_0(k; \Delta_1) \right), \quad (43)$$

$$c_{\mu\nu\lambda}^{\alpha\beta\gamma} = \frac{i}{8} \text{Tr} \left(\left\{ \frac{\partial G_0^{-1}}{\partial k_\mu}, s_\alpha \right\}_+ G_0(k; \Delta_1) \left\{ \frac{\partial G_0^{-1}}{\partial k_\nu}, s_\beta \right\}_+ \times G_0(k; \Delta_1) \left\{ \frac{\partial G_0^{-1}}{\partial k_\lambda}, s_\gamma \right\}_+ G_0(k; \Delta_1) \right), \quad (44)$$

$$d_{\mu\nu\lambda}^\alpha = -\frac{e}{4} \text{Tr} \left(\left\{ \frac{\partial G_0^{-1}}{\partial k_\mu}, s_\alpha \right\}_+ G_0(k; \Delta_1) \frac{\partial G_0^{-1}}{\partial k_\nu} \times G_0(k; \Delta_1) \frac{\partial G_0^{-1}}{\partial k_\lambda} G_0(k; \Delta_1) \right), \quad (45)$$

where Tr denotes trace over all Pauli matrices and integration over frequencies and momenta. We now need to evaluate these coefficients and we begin with $b_{\mu\nu\lambda}^{\alpha\beta}$ and $c_{\mu\nu\lambda}^{\alpha\beta\gamma}$. We note that for $b_{\mu\nu\lambda}^{\alpha\beta}$, all the coefficients with $\alpha \neq z$ and $\beta = z$ or vice versa vanish when we take trace over Pauli matrices in spin-space. The same line of reasoning shows that only the coefficients $c_{\mu\nu\lambda}^{\alpha\alpha z}$ or $c_{\mu\nu\lambda}^{xyz}$ can be non-zero. Further it is easy to see that only $d_{\mu\nu\lambda}^z$ has non-vanishing trace. Thus the only non-vanishing

coefficients can be written as

$$b_{\mu\nu\lambda}^{xx/yy} = -\frac{1}{2} \text{Tr} \left(\frac{\partial G_0^{-1}}{\partial k_\mu} G_0(k; -\Delta_1) \frac{\partial G_0^{-1}}{\partial k_\nu} G_0(k; \Delta_1) \times \frac{\partial G_0^{-1}}{\partial k_\lambda} G_0(k; \Delta_1) \right) = c_{\mu\nu\lambda}^{xyz}, \quad (46)$$

$$b_{\mu\nu\lambda}^{xy} = -\frac{i}{2} \text{Tr} \left(s_z \frac{\partial G_0^{-1}}{\partial k_\mu} G_0(k; -\Delta_1) \frac{\partial G_0^{-1}}{\partial k_\nu} G_0(k; \Delta_1) \times \frac{\partial G_0^{-1}}{\partial k_\lambda} G_0(k; \Delta_1) \right) = c_{\mu\nu\lambda}^{xxz} = c_{\mu\nu\lambda}^{yyz} = -b_{\mu\nu\lambda}^{yx}, \quad (47)$$

$$b_{\mu\nu\lambda}^{zz} = -\frac{1}{2} \text{Tr} \left(\frac{\partial G_0^{-1}}{\partial k_\mu} G_0(k; \Delta_1) \frac{\partial G_0^{-1}}{\partial k_\nu} G_0(k; \Delta_1) \times \frac{\partial G_0^{-1}}{\partial k_\lambda} G_0(k; \Delta_1) \right) = a_{\mu\nu\lambda}/e^2, \quad (48)$$

$$d_{\mu\nu\lambda}^z = -\frac{e}{2} \text{Tr} \left(s_z \frac{\partial G_0^{-1}}{\partial k_\mu} G_0(k; \Delta_1) \frac{\partial G_0^{-1}}{\partial k_\nu} G_0(k; \Delta_1) \times \frac{\partial G_0^{-1}}{\partial k_\lambda} G_0(k; \Delta_1) \right) = c_{\mu\nu\lambda}^{zzz}. \quad (49)$$

It turns out^{8,22} that coefficients $b_{\mu\nu\lambda}^{\alpha\beta}$ also satisfy the identity $b_{\mu\nu\lambda}^{\alpha\beta} = -b_{\nu\mu\lambda}^{\beta\alpha}$. Using this, we find that the contribution of terms proportional to $b_{\mu\nu\lambda}^{xy}$ in the effective action leads to a total derivative which we ignore and those due to $c_{\mu\nu\lambda}^{\alpha\alpha z}$ vanish identically. Further one can use the fact that the fields Ω_μ are pure gauge fields and hence satisfy the identity

$$\partial_\mu \Omega_\nu - \partial_\nu \Omega_\mu - \Omega_\mu \times \Omega_\nu = 0. \quad (50)$$

Using Eqs. 50 and 47, it is easy to show that all the terms proportional to $b_{\mu\nu\lambda}^{xx/yy}$ vanish. Thus finally we are left with the effective action

$$S^{(1)} = a_{\mu\nu\lambda} \int d^2r dt A_\nu \partial_\lambda A_\mu, \quad (51)$$

$$S^{(2)} = \frac{a_{\mu\nu\lambda}}{e^2} \int d^2r dt \Omega_\nu^z \partial_\lambda \Omega_\mu^z, \quad (52)$$

$$S^{(3)} = d_{\mu\nu\lambda}^z \int d^2r dt A_\nu \partial_\lambda \Omega_\mu^z. \quad (53)$$

The next task is to evaluate the coefficient $a_{\mu\nu\lambda}$, which can be done by straightforward evaluation of integrals. But before resorting to algebraic manipulation, it is easier to note that one needs $a_{\mu\nu\lambda} = e^2 \epsilon_{\mu\nu\lambda} a$ for electromagnetic gauge invariance of $S^{(1)}$, where a is given by

$$a = -\frac{1}{2} \text{Tr} \left(\frac{\partial G_0^{-1}}{\partial k_x} G_0(k; \Delta_1) \frac{\partial G_0^{-1}}{\partial k_y} G_0(k; \Delta_1) \times \frac{\partial G_0^{-1}}{\partial \omega} G_0(k; \Delta_1) \right). \quad (54)$$

Further, we find that the contribution to a in Eq. 54 is a sum of contributions from spin \uparrow and \downarrow sectors:

$a = a_\uparrow + a_\downarrow$. Whereas each of these two contributions can be finite since the Hamiltonian (Eq 32) breaks time reversal symmetry for each spin species, their sum must vanish since the total Hamiltonian for both the spin species is time reversal invariant. Thus we conclude that $a = 0$ and hence $b_{\mu\nu\lambda}^{zz} = 0$, so that graphene does not support charge Hall effect in the absence of an external magnetic field and also does not have a pure SU(2) Hopf term. However, the same argument tells us that $d_{\mu\nu\lambda}^z = -e\epsilon_{\mu\nu\lambda}d \neq 0$, since $d = a_\uparrow - a_\downarrow \neq 0$. Indeed a straightforward evaluation of a shows $a_\uparrow = -a_\downarrow = -1/2\pi$. Hence we conclude that the effective action of graphene supports a crossed Hopf term

$$S^{(3)} = \frac{e}{2\pi}\epsilon_{\mu\nu\lambda} \int d^2r dt \Omega_\mu^z F_{\nu\lambda}, \quad (55)$$

where $F_{\nu\lambda} = \partial_\nu A_\lambda - \partial_\lambda A_\nu$ is the electromagnetic field tensor. This leads to a quantized Hall spin-current (Eq. 37)

$$j_i^z = \epsilon_{ij} \frac{e}{2\pi} E_j, \quad (56)$$

where $\mathbf{E} = -\nabla A_0 - \partial_t \mathbf{A}$ is the applied electric field.

Next we introduce the Rashba term in Eq. 32. We shall restrict the analysis to the case of $\lambda_R/\Delta_1 \ll 1$ and assume that the strength of the Rashba term is not sufficient to destroy the spin-Hall phase. In the presence of such a term, the inverse of the Green function in S_0 (Eq. 34) becomes

$$G_0^{-1R} = \omega - v_F(\tau_3 k_x \sigma_x + k_y \sigma_y) - \Delta_1 \tau_z \sigma_z s_z - \lambda_R (\tau_z s_y \sigma_x - s_x \sigma_y). \quad (57)$$

One can now repeat the same analysis as described above with $G_0(k; \Delta_1)$ replaced by $G_0^R(k; \Delta_1, \lambda_R)$. Since $\partial G_0^{-1R}/\partial k_\mu$ is identical to $\partial G_0^{-1}/\partial k_\mu$, one finds that all the arguments regarding the coefficients $a_{\mu\nu\lambda}$, $b_{\mu\nu\lambda}^{\alpha\beta}$, $c_{\mu\nu\lambda}^{\alpha\beta\gamma}$, and $d_{\mu\nu\lambda}^\alpha$ remain the same and, in the end, we are left with

$$\begin{aligned} S^{(3)} &= d^R \epsilon_{\mu\nu\lambda} \int d^2 dt \Omega_\mu^z F_{\nu\lambda}, \\ d^R &= \frac{e}{2} \text{Tr} \left(s_z \frac{\partial G_0^{-1R}}{\partial k_x} G_0^R(k; \Delta_1, \lambda_R) \frac{\partial G_0^{-1R}}{\partial k_y} \right. \\ &\quad \left. \times G_0^R(k; \Delta_1, \lambda_R) \frac{\partial G_0^{-1R}}{\partial \omega} G_0^R(k; \Delta_1, \lambda_R) \right), \\ &= \frac{e}{2\pi} \left(1 - \frac{\lambda_R^2}{6\Delta_1^2} + \dots \right), \end{aligned} \quad (58)$$

where the ellipsis represent terms which are higher order in λ_R/Δ_1 , and we have obtained the last line by explicitly evaluating the matrix traces and frequency and momentum integrals in the expression of d^R . Thus we find that the spin-Hall conductivity deviates from its quantized value and equals $e(1 - \lambda_R^2/(6\Delta_1^2))/2\pi$ for $\lambda_R/\Delta_1 \ll 1$.

B. Edge states

The edge states in graphene in the absence of any external magnetic field can be analytically obtained from the Dirac Hamiltonian H (Eq. 32) for the armchair edge. Throughout this section, we shall restrict ourselves to the case $\lambda_R = 0$. The geometry we study here is that of a semi-infinite sample occupying $x > 0$ with an armchair edge at $x = 0$. For such an edge, the boundary condition demands both ψ_A and ψ_B to vanish at $x = 0$. In what follows, we construct an analytical solution for the low-energy subgap localized energy states of the graphene hamiltonian H (Eq. 32) which respects the boundary condition $\psi_A(x = 0) = 0$ and $\psi_B(x = 0) = 0$. Notice that in doing so by starting from Dirac equation, we ignore the lattice effects at the edge, which usually puts a momentum cut-off k_c above which the present description breaks down. The estimate of k_c can not be reliably done without going into numerical analysis of the lattice Hamiltonian^{11,24}.

To construct such a solution, we note that the only way to achieve the above-mentioned boundary condition is to superpose wave-functions in the K and K' points. We therefore try a normalized wavefunction of the form

$$\psi_{\text{edge}}(x, k_y) = e^{ik_y y - \kappa x} \sqrt{\kappa} \left[\begin{pmatrix} u_{As}^K \\ u_{Bs}^K \end{pmatrix} e^{i\mathbf{K}\cdot\mathbf{r}} - \begin{pmatrix} u_{As}^{K'} \\ u_{Bs}^{K'} \end{pmatrix} e^{i\mathbf{K}'\cdot\mathbf{r}} \right]. \quad (59)$$

Here $s = \uparrow, \downarrow$ denotes the spin of the electrons, \mathbf{K} and \mathbf{K}' are the wavevectors of the K and K' points in Brillouin zone of graphene, κ^{-1} denotes localization length of the edge states, and k_y denotes momenta parallel to the edge. The normalization condition $\sum_s \int dx |\psi_{\text{edge}}(x)|^2 = 1$ of the wave functions imply $\sum_s |u_{As}^{K(K')}|^2 + |u_{Bs}^{K(K')}|^2 = 1$ and the boundary condition $\psi_{\text{edge}}(x) = 0$ necessitates the condition

$$\frac{u_{As}^K}{u_{Bs}^K} = \frac{u_{As}^{K'}}{u_{Bs}^{K'}}. \quad (60)$$

From Eqs. 32 and 59, it is easy to see that the wavefunctions (u_{As}^K, u_{Bs}^K) and $(u_{As}^{K'}, u_{Bs}^{K'})$ satisfy Schrodinger equations

$$\begin{pmatrix} \text{sgn}(s)\Delta_1 & iv_F(\kappa - k_y) \\ iv_F(\kappa + k_y) & -\text{sgn}(s)\Delta_1 \end{pmatrix} \begin{pmatrix} u_{As}^K \\ u_{Bs}^K \end{pmatrix} = E \begin{pmatrix} u_{As}^K \\ u_{Bs}^K \end{pmatrix}, \\ \begin{pmatrix} -\text{sgn}(s)\Delta_1 & -iv_F(\kappa + k_y) \\ -iv_F(\kappa - k_y) & \text{sgn}(s)\Delta_1 \end{pmatrix} \begin{pmatrix} u_{As}^{K'} \\ u_{Bs}^{K'} \end{pmatrix} = E \begin{pmatrix} u_{As}^{K'} \\ u_{Bs}^{K'} \end{pmatrix}, \quad (61)$$

where $\text{sgn}(s) = +(-)$ for $s = \uparrow (\downarrow)$. Solving the

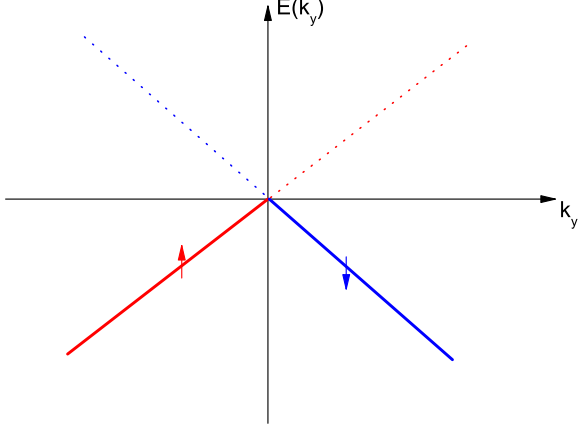


FIG. 4: Edge states near an armchair edge in graphene. The solid and dotted lines show occupied and empty spin-up (red) and spin-down (blue) edge states. An equal occupation of the spin-up and spin-down edge states result in cancellation of charge current.

Schrodinger's equations, one obtains

$$\frac{u_{A_s}^K}{u_{B_s}^K} = \frac{E - \text{sgn}(s)\sqrt{E^2 + v_F^2(\kappa^2 - k_y^2)}}{iv_F(\kappa - k_y)}, \quad (62)$$

$$\frac{u_{A_s}^{K'}}{u_{B_s}^{K'}} = -\frac{E + \text{sgn}(s)\sqrt{E^2 + v_F^2(\kappa^2 - k_y^2)}}{iv_F(\kappa + k_y)}, \quad (63)$$

$$v_F\kappa = \sqrt{\Delta_1^2 - E^2 + v_F^2 k_y^2}. \quad (64)$$

The boundary condition $\psi(x=0) = 0$ (Eq. 60) now yields the condition

$$\frac{E - \text{sgn}(s)\sqrt{E^2 + v_F^2(\kappa^2 - k_y^2)}}{E + \text{sgn}(s)\sqrt{E^2 + v_F^2(\kappa^2 - k_y^2)}} = \frac{k_y - \kappa}{k_y + \kappa}. \quad (65)$$

Together with Eq. 64, this gives us localized states at the edge with energy $E(k_y)$ and localization length κ^{-1}

$$E(k_y) = \text{sgn}(s)v_F k_y, \quad \kappa^{-1} = \frac{v_F}{\Delta_1}, \quad (66)$$

$$\begin{aligned} \psi_{\text{edge}}(x, k_y) &= \frac{\sqrt{\kappa}}{2} e^{ik_y y - \kappa x} e^{-i\text{sgn}(s)\pi/4} \\ &\times \left[\begin{pmatrix} 1 \\ i\text{sgn}(s) \end{pmatrix} e^{i\mathbf{K}\cdot\mathbf{r}} - \begin{pmatrix} 1 \\ i\text{sgn}(s) \end{pmatrix} e^{i\mathbf{K}'\cdot\mathbf{r}} \right]. \end{aligned} \quad (67)$$

Notice that the analysis of the Dirac Hamiltonian predicts linear dispersion of edge states for all k_y . This is clearly an artifact throwing out the lattice and so we would expect the results to break down at momenta $k_y^{\text{max}} = k_c$, as commented earlier.

The edge states, in contrast to their chiral superconducting counterparts, have *opposite* group velocities for spin-up and spin-down electrons as shown in Fig. 4. Further, in a transverse momentum state k_y , the edge states carry a charge current

$$j_y(k_y) = ev_F n(k_y) \langle \psi_{\text{edge}} | \sigma_y | \psi_{\text{edge}} \rangle = e \text{sgn}(s) v_F n(k_y), \quad (68)$$

where we have neglected the small $O(\kappa/|K_x - K'_x|)$ contributions. Note that the charge current is carried with the group-velocity $v_g = \text{sgn}(s)v_F$ and thus has opposite direction for opposite spins. Hence these edge states do not carry a net charge current for equal occupation of spin-up and spin-down electron states, but carry a net spin-current circulating along the edge. Note that an estimation of the total spin-current carried by the edge requires a knowledge of the states at large k_y , and hence can not be reliably done within this formalism. However, we would like to stress that the low-energy linear dispersion of the edge states with opposite group velocities for spin-up and spin-down electrons agrees well with the numerical calculations of Refs.^{11,12}.

IV. DISCUSSION

The most direct way of detecting spin/charge current at the edge is to create a population imbalance of the spin-up and spin-down edge states. Such experiments has been performed for quantum Hall samples in Ref. 25 and suggested for ruthenates in Ref. 18. The idea is to apply a magnetic pulse $\mathbf{B}(t)$ to the edge of a chiral triplet superconductor with $\mathbf{B} \parallel \mathbf{d}$. This creates an imbalance in the population of the spin-up and spin-down edge states leading to local magnetization which travels with the group velocity v_e . The magnetic moment due to this spin imbalance can be detected by a squid magnetometer as pointed out in Ref. 18. The spin structure of the edge states can also be verified since a similar experiment with $\mathbf{B} \perp \mathbf{d}$ will produce a null result. This feature distinguishes the triplet chiral superconductors from their singlet counterparts where the direction of the applied pulsed magnetic field does not matter.

A similar experiment can be performed to verify the edge state picture for graphene. Let us consider creating a population imbalance for sub-gap edge states in graphene by applying a magnetic field pulse B along z . In the absence of spin-flip scattering and for $B \leq \Delta_1$ where the states in the bulk are gapped, such an imbalance would persist and lead to a circulating quantized charge current. The spin-flip scattering rate in graphene is expected to be small since the Rashba coupling $\lambda_R \simeq 0.5\text{mK}$ is small compared to the spin-orbit gap $\Delta_1 \simeq 1.2\text{K}$, and thus we expect the population imbalance and hence the charge current to persist for a sufficiently long time²⁶. The magnitude of this charge current depends only on the population imbalance between up and down spin low-energy subgap electrons and

hence, unlike the edge spin-current, can be reliably estimated from the edge state picture developed in Sec. III B. Using Eq. 68, we obtain for the magnetic pulse along z

$$I_{\text{edge}}^{\text{charge}} = ev_F \sum_{k_y} (n_{\uparrow}(k_y) - n_{\downarrow}(k_y)) = \frac{2e}{h} g\mu_B B. (69)$$

This quantized charge-current for $g\mu_B B = \Delta_1 = 1.2K$ leads to a net current of $I_{\text{edge}}^{\text{charge}} \simeq 8\text{nA}$ which can be easily detected by a setup similar to that proposed in Ref. 25. One of the central feature of the edge states in graphene is that the direction of this charge edge current depends on the direction of the applied magnetic pulse. This feature can also be detected by a time-of-flight measurement analogous to those suggested in Refs. 18,25. Alternatively, one can also selectively populate the up or down-spin edge states by spin-polarized tunneling into the edge states. The direction of the edge current measured in such a tunneling experiment would depend on the polarization of the tunneling electrons and would serve as a definitive proof of the spin-dependent velocity of the edge states.

In conclusion, we have studied the bulk and edge properties of TRS broken and TRS invariant systems such as triplet chiral superconductors and graphene. We have

shown that both the structure of the edge states and the topological terms in the bulk effective action of these systems depend crucially on whether TRS is preserved or not. For TRS broken systems such as triplet chiral superconductor, the edge states carry a net charge current and the bulk action contains a SU(2) Hopf leading to a spin-Hall current in response to the gradient of applied Zeeman magnetic field. We have also shown that both the edge and the bulk spin-Hall current of triplet superconductors, in response to an applied Zeeman field \mathbf{B} , depend crucially on whether $\mathbf{B} \parallel \mathbf{d}$ or $\mathbf{B} \perp \mathbf{d}$. This is a consequence of broken spin-rotational symmetry in these systems and serves as a distinguishing feature of triplet chiral superconductors from their singlet counterparts. In contrast, for TRS invariant systems such as graphene, the edge states carry a net spin current while the bulk action contains a crossed Hopf term leading to a spin-Hall current in response to an external electric field. We have also suggested experiments to verify our some of our results.

KS thanks V.M. Yakovenko and H-J. Kwon for earlier collaborations on related projects. RR thanks M. Stone and E. Fradkin for useful discussions and University of Illinois Research Board for support.

-
- ¹ A.J. Leggett, Rev. Mod. Phys. **47**, 331 (1975).
² A.P. Mackenzie and Y. Maeno, Rev. Mod. Phys. **75**, 657 (2003).
³ T. Senthil, J. B. Marston, and M. P. A. Fisher, Phys. Rev. B **60**, 4245 (1999)
⁴ K. Sengupta, H-J Kwon, and V.M. Yakovenko, Phys. Rev. B **65**, 104504 (2002)
⁵ A. Furusaki, M. Matsumoto, and M. Sigrist, Phys. Rev. B **64**, 054514 (2001).
⁶ M. Matsumoto and R. Heeb, Phys. Rev. B **65**, 014504 (2002)
⁷ J. Goryo, J. Phys. Soc. Jap. **69**, 3501-3504 (2000).
⁸ G.E. Volovik and V. M. Yakovenko, J. Phys. Cond. Mat. **1**, 5263 (1989); G.E. Volovik, A. Solov'ev, and V.M. Yakovenko, JETP Lett. **49**, 65 (1989); For a review, see G.E. Volovik, *Exotic Properties of Superfluid ³He* (World Scientific, New Jersey (1993)).
⁹ M. Stone and R. Roy, Phys. Rev. B **69**, 184511 (2004).
¹⁰ S. Murakami, N. Nagaosa and S-C. Zhang, Science **301**, 1348 (2003); J. Sinova *et al*, PRL **92**, 126603 (2004).
¹¹ C. L. Kane and E. J. Mele, Phys. Rev. Lett. **95**, 226801 (2005)
¹² F. D. M. Haldane, Phys. Rev. Lett. **61**, 2015 (1988)
¹³ L. Sheng, D. N. Sheng, C. S. Ting, and F. D. M. Haldane Phys. Rev. Lett. **95**, 136602 (2005).
¹⁴ C. L. Kane and E. J. Mele, Phys. Rev. Lett. **95**, 146802 (2005).
¹⁵ V. M. Yakovenko, Phys. Rev. Lett. **65**, 251 (1990)
¹⁶ K.K. Ng and M. Sigrist, EuroPhys. Lett. **49**, 473 (2000).
¹⁷ C.R. Hu, Phys. Rev. Lett. **72**, 1526 (1994)
¹⁸ H-J. Kwon, V.M. Yakovenko, and K. Sengupta Synthetic Metals **133-134**, 27 (2003)
¹⁹ G.E. Volovik, JETP Lett. **55**, 368 (1992).
²⁰ M. A. Tanatar *et al.*, Phys. Rev. Lett **86**, 2649 (2001); K. Izawa *et al. ibid* **86**, 2653 (2001); F. Laube *et al., ibid* **84**, 1595 (2000); Z. Q. Mao *et al. ibid* **87**, 037003 (2001).
²¹ R. Roy, cond-mat/0603271 (unpublished).
²² K. Sengupta and V. M. Yakovenko, Phys. Rev. B **62** 4586 (2000).
²³ H.Y. Kee, Y.B. Kim and K. Maki, Phys. Rev. B **61**, 3584 (2000).
²⁴ L. Brey and H. A. Fertig, cond-mat/0602505 (unpublished); N. Sinitsyn *et al.*, cond-mat/0602598 (unpublished).
²⁵ R.C. Ashoori *et al.*, Phys. Rev. B **45**, 3894 (1992); G. Ernst *et al.* Phys. Rev. Lett. **79**, 3748 (1997).
²⁶ D.A. Abanin, P. Lee, and L.S. Levitov, cond-mat/0602645 (unpublished); N. M. R. Peres, F. Guinea, and A. H. Castro Neto, PRB **73**, 125411 (2006).